Journal of Hydrology 568 (2019) 1105–1117

Contents lists available at ScienceDirect

Journal of Hydrology

journal homepage: www.elsevier.com/locate/jhydrol

Research papers

The response of piezometric levels in Portugal to NAO, EA, and SCAND climate patterns

Maria C. Neves[a,b,*], Sonia Jerez[c], Ricardo M. Trigo[b]

[a] Universidade do Algarve, FCT, Campus de Gambelas, 8005-139 Faro, Portugal
[b] Instituto Dom Luiz (IDL), Faculdade de Ciências da Universidade de Lisboa, 1749-016 Lisbon, Portugal
[c] Department of Physics, University of Murcia, 30100 Murcia, Spain

ARTICLE INFO

This manuscript was handled by Corrado Corradini, Editor-in-Chief, with the assistance of Mohsen M. Sherif, Associate Editor

Keywords:
Groundwater levels
Climate variability
EA
NAO
SCAND
Portugal

ABSTRACT

Under the increasing risk of water scarcity, aquifer management strategies can take advantage of a deeper knowledge about the natural long-term fluctuations driven by climate patterns. This study examines the links between major large-scale atmospheric circulation modes and inter-annual to decadal oscillations in groundwater levels in Portugal. Precipitation and piezometric records (1987–2016) from two aquifer systems, Leirosa-Monte Real in the north and Querença-Silves in the south, are analyzed using wavelet transform methods and singular spectral analysis. Wavelet coherences computed between hydrologic time series and the North Atlantic Oscillation (NAO), East Atlantic (EA) and Scandinavia (SCAND) climate patterns show non-stationary relationships that are nonetheless consistent in distinct period bands. The strongest covariability occurs in the 6–10 years band for NAO, in the 2–4 years band for EA (especially after 1999) and in the 4–6 years band for SCAND (mainly after 2005). NAO is the mode playing the most relevant role with a stronger influence in the south (60% on average) than in the north (40% on average). The relatively higher frequency (< 5 year period) contributions of EA and SCAND are difficult to set apart but their joint impact accounts for approximately 20% and 40% of the total variance of groundwater levels in the south and north of the country, respectively. Wavelet coherence patterns also expose transitive couplings between NAO, EA and SCAND. Often, coupled phases between climate modes mark abrupt transitions in synchronization patterns and shifts in the time-frequency domain. Extremes in groundwater storage coincide with anti-phase NAO and EA combinations: maximum piezometric levels occur during NAO-EA+ (coincidentally also SCAND+) phases while minimum levels occur during NAO+EA− phases.

1. Introduction

Evidence that climate change has already begun and will continue to alter the water cycle, resulting in summertime drying trends and increased risk of drought, is compelling in Portugal (Guerreiro et al., 2017a). This situation directly affects the availability and dependency on groundwater resources, which are the source of 45–65% of the total fresh water demands in the country (Ribeiro and da Cunha, 2010). The persistence of much lower than normal precipitation and higher than normal temperature has been causing exceptionally high evapotranspiration, soil moisture deficit and depleted surface water reservoirs (IPMA, 2017; SNIRH, 2017). The year 2017 was among the 4 driest since 1931 (all 4 occurred after 2000) and drops of more than 40% in water storage were recorded on most reservoirs and dams across the country. Because of its buffer capacity, it is likely that water demand and supply will increasingly depend on groundwater, especially during summertime when tourism inflates significantly the number of people in many coastal areas of Portugal. To sustain groundwater use under increasing demand, aquifer management strategies ought to account for natural long-term hydrologic fluctuations. The identification of their driving climate patterns would help to understand, foresee, project and, finally, better manage them.

Trends in European precipitation and temperature are linked with the phases of major large-scale atmospheric circulation modes, namely the North Atlantic Oscillation (NAO), the eastern Atlantic pattern (EA) and the Scandinavian pattern (SCAND) (Comas-Bru and Mcdermott, 2013; Moore et al., 2013). In the north Atlantic these patterns control the trajectory of frontal systems during the extended winter season (Trigo et al., 2008), which in turn are responsible for most of the precipitation in western Iberia (Belo-Pereira et al., 2011). Many

* Corresponding author.
E-mail address: mcneves@ualg.pt (M.C. Neves).

https://doi.org/10.1016/j.jhydrol.2018.11.054
Received 30 July 2018; Received in revised form 16 November 2018; Accepted 19 November 2018
Available online 23 November 2018

climatological studies have established the great influence of NAO on the European climate (Hurrell et al., 2003; Hurrell and Van Loon, 1997). In western Iberia, in particular, NAO has been shown to be the main large-scale phenomenon controlling winter precipitation, river flow and surface water storage (García-Herrera et al., 2007; Jerez et al., 2013; Trigo et al., 2004). Still, recent studies found that the phases of both EA and SCAND not only have a straight impact on local conditions but also modulate the location and strength of the NAO dipole, thus causing non-stationarity on its local fingerprint (Comas-Bru and Mcdermott, 2013; Moore et al., 2013).

The links between other climate patterns (e.g. El Niño–Southern Oscillation, Pacific Decadal Oscillation, Artic Oscillation) and low frequency (inter-annual and decadal) oscillations in groundwater levels have been abundantly demonstrated in several parts of the world (Asoka et al., 2017; Gurdak et al., 2007; Kuss and Gurdak, 2014; Tremblay et al., 2011; Venencio and García, 2011). Examples of such studies in Europe focused primarily on the influence of NAO (De Vita et al., 2012; Holman et al., 2011). In Iberia, despite the important role played by groundwater in water supply, the influence of climatological cycles on aquifers has only been addressed locally in southern Spain (Andreo et al., 2006; Luque-Espinar et al., 2008) and thus, remains largely unexplored.

The primary aim of this study is to examine the impact of leading modes of atmospheric circulation, also called teleconnection patterns, on the variability of aquifer water levels in Portugal (western Iberia). Although the impact of these patterns in precipitation is well known in this area, their fingerprint on groundwater levels can not be straightforwardly inferred because soil type and depth of water table control the damping processes in the vadose zone, resulting in frequency-dependent preservation of climate signals on groundwater levels fluctuations (Dickinson et al., 2014, 2004; Velasco et al., 2017). The differential influence of geology and climate on the piezometry of the Querença-Silves (QS) karst aquifer has been examined by Neves et al. (2016). The authors suggested that the 3.2, 4.3, 6.5, and 2.6-year oscillations identified in the QS aquifer were due to natural recharge rates associated with the NAO climate cycle, but did no attempt to demonstrate this relationship. This work completes the previous study and presents the first analysis of piezometric levels in Portugal aiming to demonstrate and quantify their dependence on NAO, EA and SCAND patterns.

Finally, we test if there is a connection between extremes in piezometric levels and shifts in climate mode interactions. Recent studies demonstrate the advantage of examining the joint contributions of NAO, EA and SCAND on variables such as precipitation (Kalimeris et al., 2017), temperature (Hernández et al., 2015), streamflow (Steirou et al., 2017), wind-speed (Zubiate et al., 2017), renewable energy production (Correia et al., 2017; Jerez and Trigo, 2013) and net biome productivity (Bastos et al., 2016). But not only climate patterns occur in coupled modes as temporal shifts in their synchronization may prompt hydrological extremes. For instance, it has been shown that precipitation extremes observed in Australia are not a result of any single climate mode but instead are due to transient interactions amongst three climate patterns: El Niño–Southern Oscillation, Indian Ocean Dipole and Southern Annular Mode or Antarctic Oscillation (Cleverly et al., 2016). Motivated by these studies, the non-stationary relationships between climate indices and groundwater levels are investigated using wavelet transform methods and principal component analysis.

2. Atmospheric circulation and climate indices

The NAO, EA and SCAND indices used in this study were retrieved from NOAA's Climate Prediction Center (NOAA, 2017) at the monthly temporal resolution and aggregated for the winter months (DJFM). NOAA calculates these indices by rotated PCA (principal component analysis) of monthly means of the 500-mb geopotential height anomaly over the northern hemisphere. Fig. 1 displays the detrended time series of the indices treated here spanning the study period (1987–2016) alongside with the spatial patterns of the corresponding leading modes of variability of the 500-mb geopotential height anomaly. Positive and negative phases of the indices are defined by winter index values above the 3rd and below the 1st terciles, respectively.

The NAO shows up as a meridional dipole of the pressure field between Iceland and the Azores (Fig. 1a). The sign and strength of this dipole present considerable inter-annual and decadal oscillations (Hurrell and Van Loon, 1997). In its positive phase (NAO^+) high pressures dominate over the Azores and low pressures over Iceland, promoting warmer and wetter winters across northern Europe, while drier conditions prevail southward. In the opposite phase (NAO^-) westerly winds and storm tracks are shifted southward, enhancing precipitation over southern Europe. In western Iberia, the Pearson's correlation between the winter NAO and precipitation (1950–2007) is around −0.7 (Jerez et al., 2013), although this value has changed between −0.5 and −0.7 throughout the 20th century (Trigo et al., 2004). The evolution of the NAO index over time (1826–2002) shows modulated oscillations with periods around 4.8, 7.7, and 2.4 years, along with nonlinear trends (Gámiz-Fortis, 2002). However, caution is required in extrapolating these results as the relation between NAO and surface climate has been shown to be non-stationary (Vicente-Serrano and López-Moreno, 2008).

The EA pattern presents a dipole configuration similar to NAO but displaced to the southeast. In its positive phase (EA+) it exhibits a well defined low pressure centre in the north Atlantic to the west of the United Kingdon (Barnston and Livezey, 1987). The SCAND shows a primary centre of action over the Scandinavian Peninsula, where high pressures during its positive phase (SCAND+) give rise to a blocking situation over northern Europe leading to a southerly shift of the moisture fluxes advected from the Atlantic and intensified westerlies over southern Europe (Bueh and Nakamura, 2007). The impact of EA and SCAND on European precipitation have high spatial variability and are much less consistent than the influence of NAO (Trigo et al., 2008). Nonetheless, its contribution to the precipitation variability on Iberia is significant, particularly in Portugal, where EA and SCAND are reported to account for 33% and 13% of the total precipitation variance, respectively (Rodriguez-Puebla et al., 1998), albeit with large differences among the rainy months of the year (Trigo et al., 2008). Also, it has been demonstrated that EA and SCAND patterns modulate the influence of NAO by modifying the geographic positions of the NAO dipole, which suffers a southwestward migration when EA and NAO are on opposite phases, and a clockwise rotation when SCAND and NAO are on opposite phases (Comas-Bru and Mcdermott, 2013). By influencing the shape and strength of the NAO dipole, the interplay between NAO and EA affects the trajectory of the frontal systems and the transport of heat and water vapor over Europe (Bastos et al., 2016).

In the 1987–2016 period there were several anomalous precipitation events in mainland Portugal, here referred to as extreme events. Extreme events in Iberia, particularly droughts, are defined in the literature using a large number of different indices based on a wide range of meteorological or hydrological (longer time-scales) conditions (Guerreiro et al., 2017b; Lorenzo-Lacruz et al., 2013; Martins et al., 2012). By cross-referencing published results with deviations from winter precipitation in Portugal relative to the 1971–2000 normal (IPMA, 2017), we consider there were four major droughts in the studied period, namely in 1992–1994, 1998–2000, 2004–2006 and 2011–2012 (some of these droughts lasted for more than one hydrological year). Most of these drought events were associated with combined positive NAO and negative EA phases (Fig. 1b). Strengthening of NAO toward its positive phase contributed to extreme conditions in 2004–2005, although a negative EA during February and an abnormal blocking situation from mid-February to mid-March 2005 also played a role in this record-breaking drought (García-Herrera et al., 2007). Likewise, the major drought of 2011–2012 was characterized by months dominated by NAO+ and EA− (Trigo et al., 2013). On the

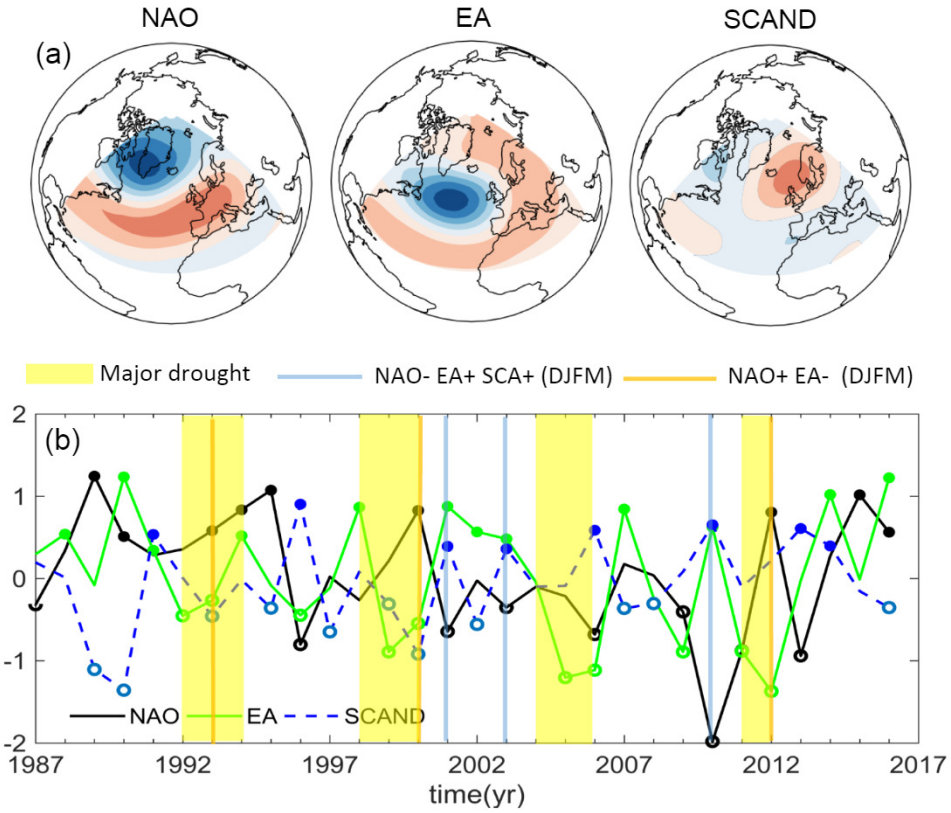

Fig. 1. NAO, EA and SCAND patterns and respective index temporal series. (a) Spatial patterns of the first three empirical orthogonal functions of the 500 hPa geopotential height over the European/Atlantic sector during winter time. (b) Time series of the winter composites (December-March) of the climate indices. Circle markers indicate positive and negative phases of each mode. Color bars indicate major droughts and anomalous wet winters associated to phase couplings. Both the patterns and the datasets were obtained from NOAA (2017).

other hand, anomalously wet winters recorded in 2001, 2003 and 2010 occurred in association with negative NAO coupled to positive EA and SCAND phases (Fig. 1b).

3. Study sites and datasets

3.1. Study sites

The Mediterranean climate prevails in Portugal. In the classification of Köppen-Geiger, the climate to the north of the country (NW of Iberia) is of type Csb, temperate with dry and mild summers. The monthly average temperature ranges between 10 and 20 °C and the total annual rainfall is about 1000 mm/year. The climate in the south (SW of Iberia) is of type Csa, temperate with dry and hot summers. The monthly average temperature ranges between 12 and 24 °C and the total annual rainfall is about 500 mm/year (IPMA, 2017). On average, about 42% of the annual precipitation in Portugal falls during the 3-month winter season (December to February) (Miranda et al., 2002). Thus, the precipitation during the winter months determines the availability of surface water resources in subsequent months. The aquifers studied here, the Leirosa-Monte Real (LM) and the Querença-Silves (QS), were selected firstly for their location (one aquifer in each climate zone, Fig. 2) and secondly by the availability and completeness of their groundwater level records.

The QS aquifer is the largest (324 km^2) and most studied groundwater reservoir in South Portugal (Hugman et al., 2012; Monteiro, 2006; Stigter et al., 2014). It is a karst aquifer mainly formed by Jurassic carbonate rocks, behaving as both a confined and unconfined aquifer system in different areas. The S. Marcos-Quarteira fault, a major regional structure inherited from the Variscan Orogeny, divides the aquifer in two compartments with distinct hydrogeological behavior (Neves et al., 2016). The region to the east of the fault is characterized by relatively high (~15%) hydraulic gradients largely controlled by topography. In contrast, the region to the west of the fault is a flat lowland area characterized by smooth piezometric isolines, predominant E-W flow, as well as comparatively higher and homogeneous values of transmissivity and water storage capacity. Groundwater discharge occurs mainly through a small number of springs located in the western limit of the aquifer. Studies focusing on the spatial distribution of recharge estimated that the average annual recharge is 45% of the rainfall (Hugman et al., 2012). Recently, a numerical modeling study on the impact of climate-change scenarios on this aquifer shows that wells within 6 km of the coast may be at risk of water quality degradation due to seawater intrusion (Hugman et al., 2017).

The Leirosa-Monte Real is one of the few aquifer systems in the NW zone that has not suffered from piezometric declining trends due to over-exploitation in the last decades (Ribeiro and da Cunha, 2010). It extends along a coastal strip up to 8 km wide that gently slopes down to the east and occupies an area of 218 km^2. The aquifer is classified as a porous, multilayer system, mainly formed by plio-pleistocene sands that cover sub-horizontal deposits of pre-Miocene sandy clays and Mesozoic calcareous loams (SNIRH, 2017). The sediments fill depressions between diapiric structures and form sequences varying between 25 and 250 m thick. The groundwater flow is directed towards the Atlantic Ocean, and sometimes, in the morphologically depressed areas, the water table rises up creating ephemeral lagoons. The aquifer recharge is estimated to be around 30% of precipitation (Almeida et al., 2000).

3.2. Datasets

The groundwater level records were required to have a monthly temporal resolution, be continuous for at least 30 years and be unaffected by pumping. Two piezometers in each aquifer, with records fulfilling these requirements, were selected to represent the range of observed hydrogeological conditions. Carriço and Benafim are located at relatively high land elevation, while Lavos and Silves are located near the discharge areas (Fig. 2). The monthly groundwater level time series span from January 1987 to December 2016 and were obtained from the Portuguese National System for Water Resources Information SNIRH site (SNIRH, 2017).

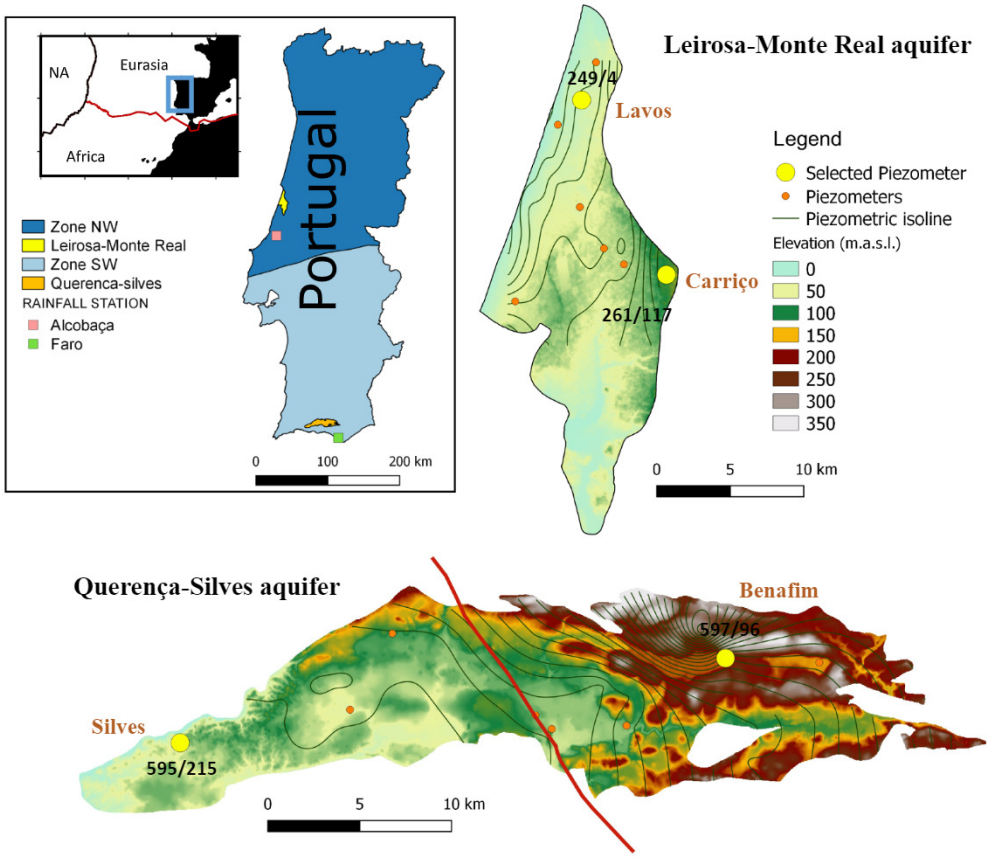

Fig. 2. Map showing the location of the Leirosa-Monte Real (LM) and Querença-Silves (QS) aquifers, the zonation of the mean annual precipitation in Portugal (NW and SW zones), the terrain elevation and the locations of piezometers and meteorological stations. Numbers indicate the studied piezometer identification code. Carriço and Benafim are located at relatively high elevation above sea level while Lavos and Silves are located close to the discharge area. The piezometric isolines have been computed from the average hydraulic heads observed at all piezometers available in the area using the krigging linear method of interpolation.

Precipitation data were obtained from two weather stations operated by the Portuguese Meteorological and Ocean Office (IPMA, 2017), Faro and Alcobaça (Fig. 2). These weather stations are 50 km away from the aquifers but are the closest available with continuous records in the 1987–2016 period. Concerns on the spatial representativeness of the weather station data lead us to consider other precipitation datasets (Sun et al., 2018) such as ERA-Interim (ERA-I), a global atmospheric reanalysis relying on both observations and model-based forecasts (80 km spatial resolution) available from the European Center for Medium-Range Weather Forecasts (ECMWF, 2017). ERA-I has been shown to perform quite well in western Iberia when compared to data based on meteorological stations and rain gauges (Belo-Pereira et al., 2011) and the two datasets are indeed well correlated at our study sites (Pearsońs coefficients > 0.8 at both Faro and Alcobaça). However, the datasets also show some discrepancies such as a systematic bias at Faro which require further investigation. A future study, currently in preparation, will analyze these discrepancies but the preliminary results obtained so far made us confident in the suitability of the weather station data for the purpose of this work.

4. Methods

Several analytical techniques were employed to characterize the temporal structure and the periodic components of the time series (continuous wavelet transform, wavelet principal component and singular spectral analysis), as well as the temporal correlations between them (wavelet coherence). Each technique has its own purpose and advantages and their combination provides a robust picture of the links between groundwater levels, precipitation, and the climate indices. Quite often wavelet and singular spectral analysis are both applied to the same climatic series (e.g. Moreno et al., 2018) with the latter designed to evaluate short, noisy and chaotic signals while the former is better suited to deal with aperiodic and quasi-periodic data. Typical pre-processing steps such as searching for outliers, interpolation for estimating missing values, detrending and normalization by standard deviations were carried out before the analysis.

4.1. Temporal correlations

The links between groundwater level and monthly precipitation are examined using linear regression, with a two-tailed significant *t*-test at the 95 percent confidence level. First, monthly precipitation times series are transformed into cumulative departures, detrended and normalized using the methods described by Hanson et al. (2004). Lag correlation analysis, which gives the correlation coefficient as a function of the lag between two time series, is also used to identify the lag of maximum correlation between the causal process (precipitation) and the aquifer system response (groundwater level).

4.2. Continuous wavelet transform

The continuous wavelet transform (CWT) is appropriate to analyze non-stationary signals that have temporal variations in both amplitude and frequency. Its main advantage over classical spectral methods is that it is able to reveal the time evolution of the dominant modes of variability, being as such specially tailored for the detection of localized or intermittent events. The CWT is defined as the convolution of the signal with a scaled and translated version of the wavelet function (Daubechies, 1990). The method is implemented in MATLAB using the Morlet wavelet described in Torrence and Compo (1998). The Morlet wavelet presents several advantages over other wavelets, such as the equivalence between scale and the equivalent Fourier period (Sang, 2013). We use 29 scales (monthly sampling rate and 4 sub-octaves per scale) which allows us to analyze periods ranging from 2 months to 21 years. The wavelet spectrum depicts the temporal distribution of the power (variance) of the time series as a function of period (scale), over

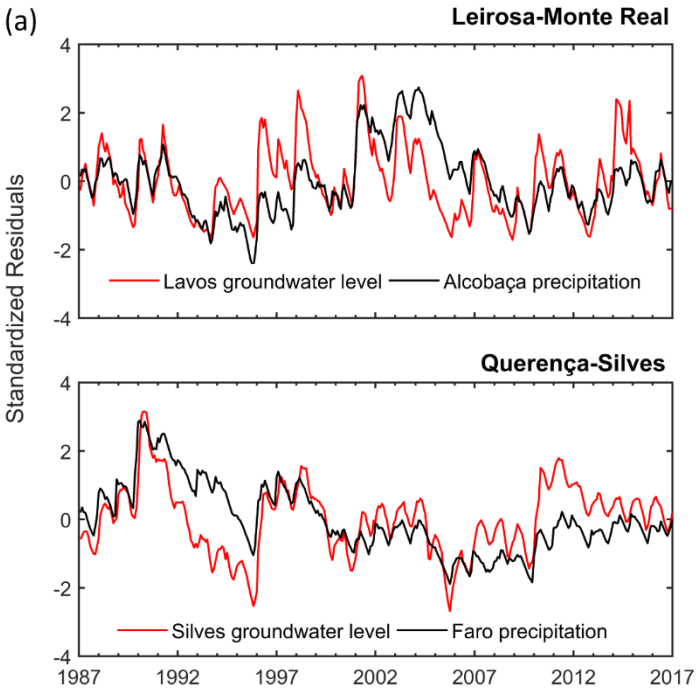

Fig. 3. (a) Monthly values of normalized residuals of cumulative departure of precipitation at Alcobaça (LM aquifer) and Faro (QS aquifer) weather stations and normalized residuals of groundwater level time series (one piezometer per aquifer) (b) Linear correlations between normalized residuals (number indicates Pearson's correlation coefficient).

the 30 years of analysis. The spectrum is normalized by $1/\sigma^2$, where σ^2 is the variance of the time series. The 5% significant levels are computed using a Chi-square test against a red noise spectrum as the null hypothesis. The cone of influence delimits the regions where the edge effects, due to zero padding, make the results less reliable.

4.3. Wavelet coherence

The wavelet coherence (WTC) is used to identify time-localized common oscillatory behavior in two time series. Its definition is similar to a localized correlation coefficient between two CWT in time-frequency space (Torrence and Webster, 1998). The WTC in this study is computed at the 95% confidence level using the algorithm described in Grinsted et al. (2004). The phase relationship is shown by the orientation of the arrows in regions of high coherence. For example, horizontal arrows from left to right indicate in-phase relationships. Areas above the 5% significant level indicate locked phase behavior but not necessarily common high power. Regions in time-frequency space with large common power and consistent phase relationship are likely to possess a causality between the time series.

4.4. Wavelet PCA

Wavelet Principal Component Analysis (wPCA) is suited to detect patterns that are concealed or not visible in raw data (Katul and Parlange, 1995). The method is implemented in Matlab (wavelet toolbox) using two processing steps to extract localized signal features. The first step is a Discrete Wavelet Transform resulting in the determination of approximation and detail coefficients (A5 and D5-D1). We employed a time series decomposition into five levels (i.e. 2^5 scales) using a 2nd order symlet ('sym2' wavelet) and checked that other choices of the number of levels or wavelets (e.g. 2nd order Daubechies) did not alter the main conclusions. The second step involves a principal component analysis applied to the matrix of approximation and details, which allows finding the projections of the filtered signal maximizing the variance (i.e. their principal components or PCs). Partial reconstructions of a selected number of retained principal components provide simplified versions of the original signal. In this study, we present the first three principal components (PC1, PC2 and PC3) along with the percentage of the total variance explained by each of them.

Subsequently to wPCA, we have computed temporal correlations between the PCs of groundwater levels and the climate indices (NAO, EA and SCAND) using Spearman's rank coefficients.

4.5. SSA of groundwater level

The singular spectral analysis (SSA) is a form of principal component analysis used to extract the dominant frequencies in short and noisy time series. The advantage over harmonic analysis through a Fourier transform is that the fitted functions are not defined a priori, but are based on structures determined through eigenanalysis. Following the methods outlined by Dettinger et al. (1995) and Hanson et al. (2004) the calculations are carried out by diagonalizing a lagged covariance matrix (Vautard et al., 1992). We compute the SSA using the Hydrologic and Climate Analysis Toolkit (Dickinson et al., 2004) with window lengths of 60 and 30 months to capture periods longer and shorter than 5 years, respectively. In any case the window length is less than 1/5 of the time series length as recommended by Ghil et al. (2002). The relative contributions of the most significant periodic components to the total variance of groundwater levels (determined through SSA) are, in the end, compared to the wPCA results.

5. Results

5.1. Precipitation versus groundwater level

The relation between precipitation and groundwater level is illustrated at each site using a single piezometer. The results for other piezometers are similar but not shown since it is not the purpose of this study to give an exhaustive representation of the heterogeneity in each aquifer. Fig. 3a shows that there is an almost instantaneous response between precipitation and hydraulic head variations (the time lag of maximum correlation is zero) consistent with the permeable nature of the sediment cover and the shallow depth of the water table, at both Lavos and Silves (Table 1). The correlation between precipitation and groundwater level is also similar at both sites (Pearsońs coefficient ~ 0.6) (Fig. 3b).

The wavelet power spectra of precipitation and groundwater levels

Table 1
Summary of hydrologic and statistical parameters of the data (1987–2016).

Piezometer	Topographic Elevation (m a.s.l.)	Mean piezometric level (m)	Range of Water level Fluctuations (m)	Memory effect (months)
249/4 Lavos	25.0	23.1	22–23	13
261/117 Carriço	83.0	41.8	37–49	15
595/215 Silves	63.8	5.1	1–10	15
597/96 Benafim	182.5	123.8	117–138	13

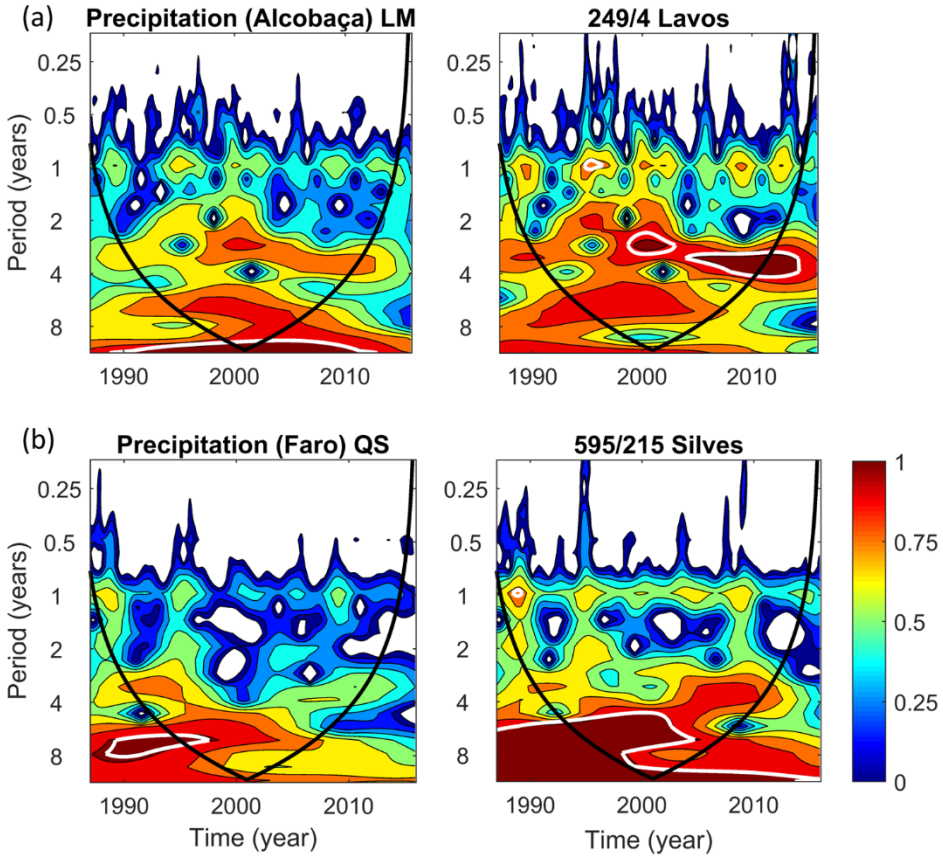

Fig. 4. Wavelet power spectra of precipitation and groundwater level records at (a) Leirosa-Monte Real and (b) Querença-Silves. The white contours enclose regions of greater than 95% confidence levels. The black lines delimit the cone of influence where the edge effects become important.

are compared at each aquifer, and across aquifers, in Fig. 4. Although there are some notable differences in mid-frequency timing across aquifers, the CWT plots are otherwise similar. An important common aspect that emerges from these spectra is the power concentration in two distinct bands, the first concentrated in the 4–8 years band, most intense before 2005, and the second occurring in the 2–4 years band from 2000 onwards. The variability modes having enough persistence and amplitude to be statistically significant (within white contours) peak at different frequencies in the two study sites. In the north (Fig. 4a) the power is concentrated in the 2–4 years band while in the south (Fig. 4b) the variance peaks in the 4–8 years band. At smaller scales, one can observe several scattered peaks at periods of 1 year. The strongest patches occur in 1990, 1996, 2000 and 2010, which were anomalously wet years. It is also noteworthy the strong attenuation of power, or lack in variance, in the 1–2 year band centered on 2004, but extending for almost a decade. This anomaly can be attributed to the outstanding drought that affected the Iberian Peninsula in 2004–2005.

5.2. Links between climate indices, precipitation and groundwater level

Fig. 5 (LM aquifer) and Fig. 6 (QS aquifer) show the wavelet coherence between climate indices and precipitation or groundwater levels. In order to relate climatic extreme events and climate pattern indices, vertical lines marking the main droughts in Portugal have been drawn over the WTC plots (the 2011–2012 event was excluded for being too close to the cone of influence). The lines divide the plots into four time windows with distinctive coherence patterns, suggesting that extreme events indeed mark, as a consequence of, abrupt re-organizations of climate variability modes. At each aquifer, results for two piezometer locations intend to demonstrate the effect of spatially varying hydrogeological conditions.

Despite local differences, there is a great deal of similarity in coherence patterns across hydrological responses to a given climate index (along columns). At both study sites (Fig. 5 and Fig. 6) SCAND is the index having the most widespread influence, presenting statistically significant patches of coherence at several multiannual periodicities (especially between 1999 and 2005). Each climate index shows consistent phase-relationships at characteristic periods (although sometimes restricted to a given time window): NAO at periods of 6–10 years (especially in the south, Fig. 6), EA at periods of 2–4 years (especially after 1999, Fig. 5) and SCAND at periods of 4–6 years (especially after 2005, Fig. 5 and Fig. 6).

Regarding the phase angle, there is a dominant horizontal anti-phase (180°) relationship between NAO and the hydrologic time series

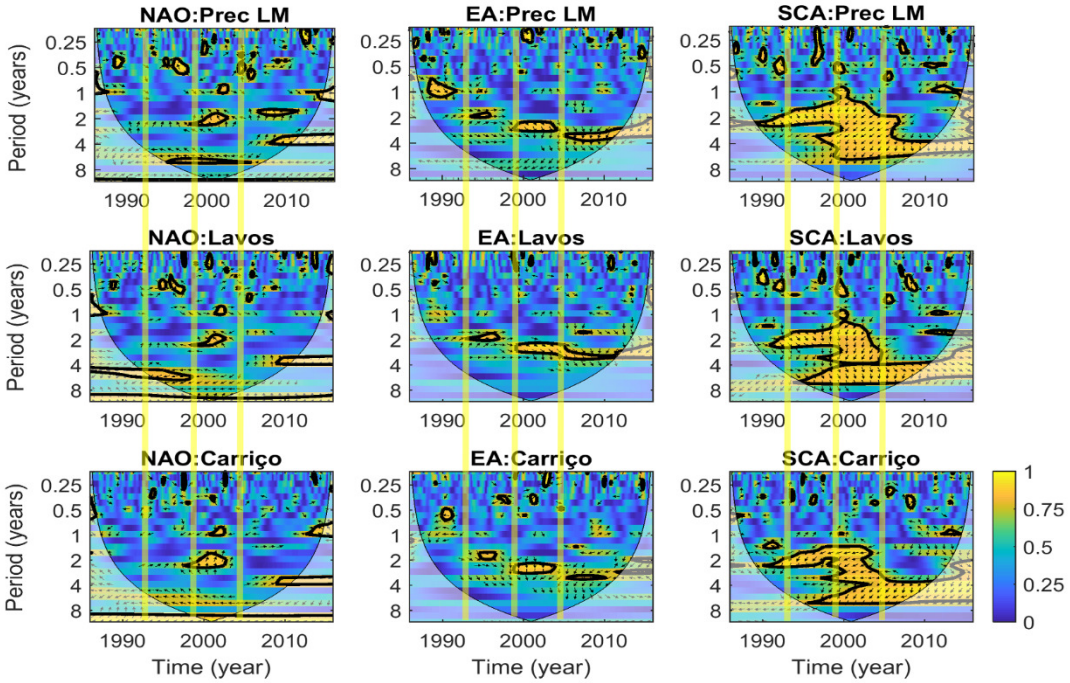

Fig. 5. Wavelet coherence in the Leirosa-Monte Real aquifer. Upper row shows the coherence between precipitation and NAO, EA and SCAND indices (vertical panels). Coherence between groundwater levels and the three indices (lower rows) are shown for two piezometers (Lavos and Carriço). Thick black lines are the 5% significance level and less intense colors indicate the cone of influence. Horizontal right-pointing (left-pointing) arrows indicate in phase (anti-phase) relationships. Vertical yellow lines indicate the major droughts identified in Fig. 1b. (For interpretation of the references to color in this figure legend, the reader is referred to the web version of this article.)

at all sites. It is well known that during NAO negative phases low-pressure systems in the north Atlantic are shifted southwards, leading to increased precipitation and increased river discharges in Iberia (Lorenzo-Lacruz et al., 2011; Trigo et al., 2008, 2004). Thus, the out-of-phase relationship is in agreement with the fact that recharge (precipitation) is negatively correlated with NAO. In contrast, EA and SCAND show preferential diagonal or downward pointing arrows that indicate some degree of lead or lag between the indices and the hydrological time series.

There are also episodes of high coherence that cannot be attributed to a single index. Such synchronized relationships reveal the impact of the coupling amongst indices. For example, synchronized coherence

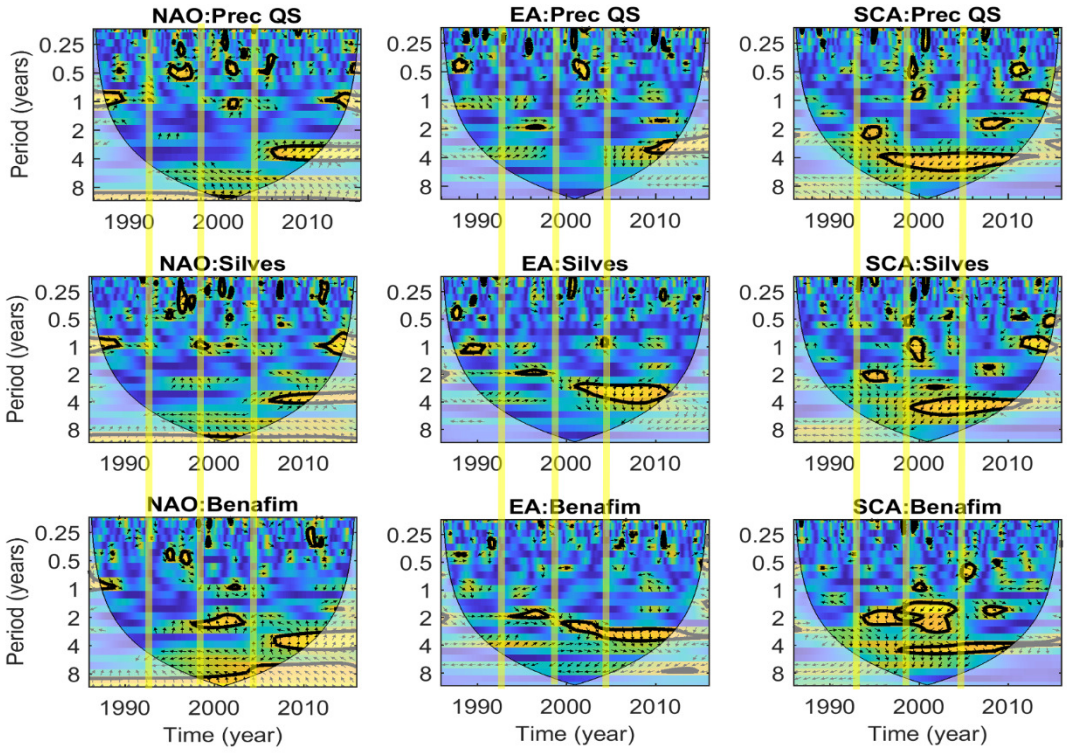

Fig. 6. Wavelet coherence of hydrologic time series and climate indices in the Querença-Silves aquifer (as Fig. 5).

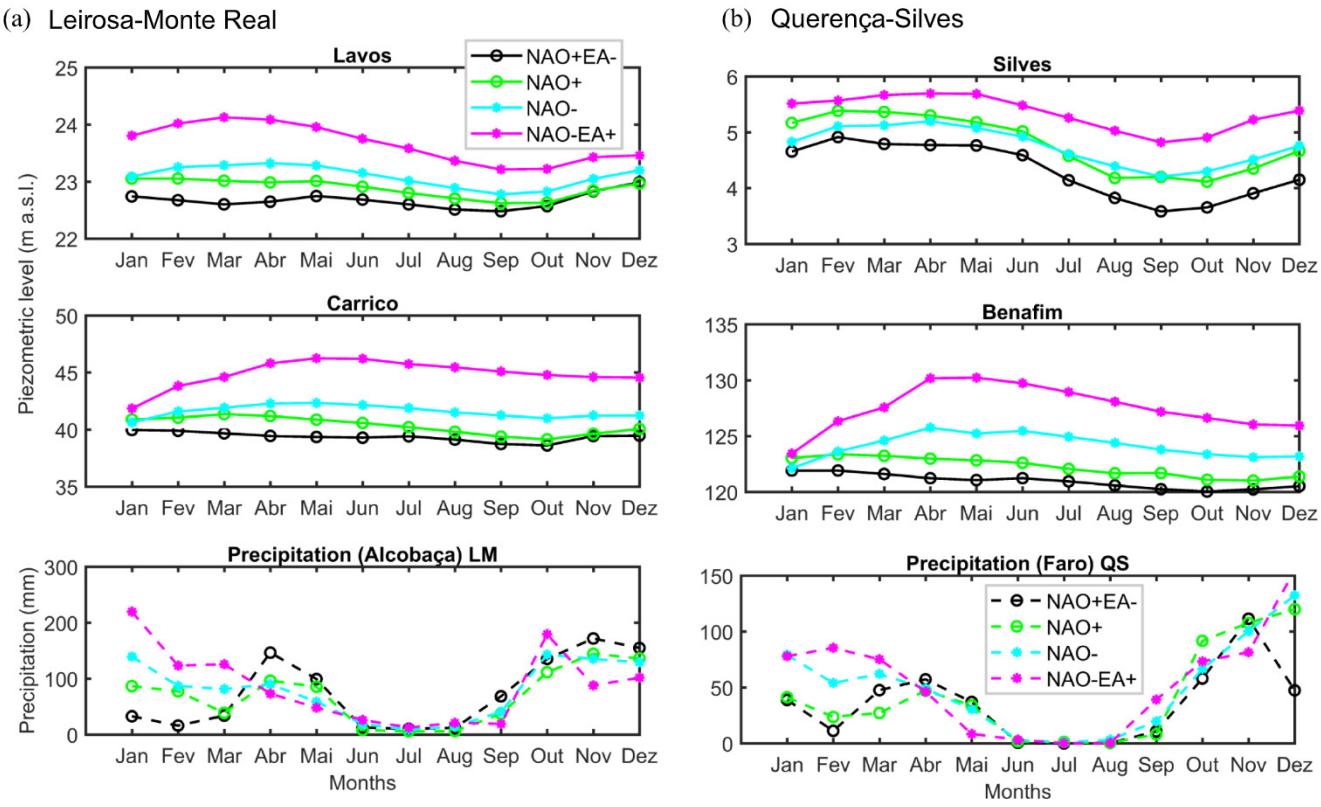

Fig. 7. Groundwater levels and precipitation per month averaged over years of positive and negative winter (December through March) NAO and NAO-EA coupled phases (a) Leirosa-Monte Real and (b) Querença-Silves aquifers.

patches at periods of around 2 years centered in 2000 (Fig. 5 and Fig. 6) correspond to coupled NAO-EA + SCAND+ phases in 2001 and 2003 (Fig. 1). The impact of coupled phases is better illustrated in Fig. 7 which displays the hydrological time series averaged over years of positive and negative phases (e.g. hydraulic head variations for NAO+ correspond to monthly values averaged over NAO+ years). More consistent relationships can be inferred from piezometric levels than from precipitation (which is highly seasonal in Iberia) owing to the buffer capacity of aquifers. Higher piezometric levels are associated with negative phases of the winter NAO, as expected. However, Fig. 7 also shows that maximum piezometric levels occur in years of NAO-EA+ (mostly coincidentally also SCAND+) combinations while minimum levels occur during NAO + EA− combinations. In fact, opposing NAO and EA phases seem to provide an envelope to all other possible phases and their combinations (not shown). Due to the limited number of years (only three) in which these conditions occur (Fig. 1) caution is required in generalizing this result. Nonetheless, these results are qualitatively similar to recent analysis of real wind power generation in Portugal, that presents its highest (lowest) values for the NAO-EA+ (NAO + EA−) combination and in between results with NAO+ and NAO- composites (Fig. 4 in Correia et al., 2017)

5.3. Quantified impacts of EA, NAO and SCAND on groundwater level

Fig. 8 shows the first three principal components of the time series obtained via wPCA. We focus on groundwater level, although the precipitation decomposition is also shown for completeness. The first principal component (PC1) accounts for nearly 50% of the total variance in groundwater levels at all sites. This component displays variable cycles of relatively long period (> 5 years) repeatedly limited by major droughts. The second and third principal components (PC2 and PC3) have shorter periods (< 5 years) and together account for 30% to 40% of the total variance. These components are hard to distinguish (for instance, PC2 at Benafim looks like PC3 at Silves) and some of their peaks coincide with anomalous wet year. This swap in the ranking of some PCs is a typical caveat of PCA analysis when two consecutive components present relatively similar values of explained variance (Trigo and Palutikof, 2001) as is the case here of PC2 and PC3 for Benafim.

Temporal correlations between complete time series of climate indices and principal components do not produce statistically significant values. However, correlations are statistically significant for a limited set of seasonal averages (Table 2). Both the summer (JJAS) and winter (DJFM) aggregates of PC1 correlate with the winter NAO, showing no association to other indices. PC2 and PC3 correlate with EA and SCAND with a delay lag of 6 months (i.e. summer aggregates correlate with winter indices). PC3 also partially correlates with NAO, especially in the south (Silves and Benafim).

We establish an association between principal components and frequencies extracted from SSA based on the period threshold separating PC1 (> 5 years) from PC2 and PC3 (< 5 years). The SSA helps to constrain the magnitude of the relative contributions of each climate mode to the overall variability (Table 3). Altogether, the climate indices account for 80% (on average) of the total variance of groundwater levels at both the LM and QS aquifers. NAO is the index playing the most relevant role in groundwater variability with a stronger influence in the south (60% on average) than in the north (40% on average). The contributions of EA and SCAND are difficult to set apart but their joint impact on variance is approximately 20% in the south and 40% in the north. Discrepancies between SSA and wPCA results are due to the presence of a NAO component in PC3. This is consistent with the previously recognized existence of NAO, EA and SCAND mode coupling.

6. Discussion

This study reinforces the role of NAO as the primary driver of

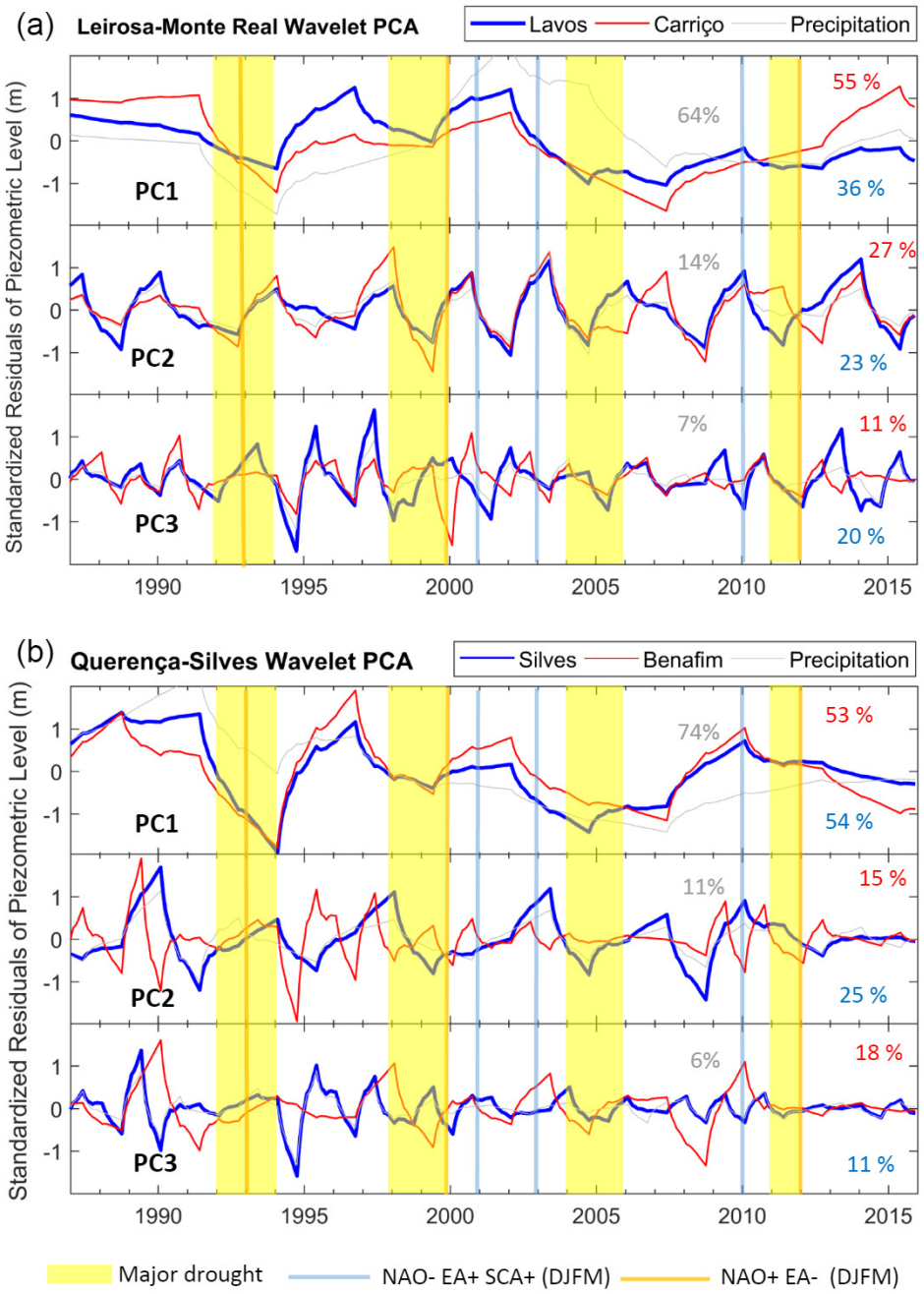

Fig. 8. First three principal components (PC1, PC2 and PC3) of groundwater levels determined from wavelet PCA and their correspondent contribution (in %) to the total variance (data for two piezometers per aquifer displayed in red and blue). Principal components of precipitation (grey) and the corresponding amount of explained variance are also shown for comparison. (a) Leirosa-Monte Real and (b) Querença-Silves aquifers. Color bars as in Fig. 1b. (For interpretation of the references to color in this figure legend, the reader is referred to the web version of this article.)

hydrological variability in Portugal, alongside with EA and SCAND. The climate-driven periodicities detected in groundwater levels compare well with results from previous studies in the Iberian Peninsula. For example, Gámiz-Fortis et al. (2008) calculated the main oscillatory components in streamflow series from the main rivers in Portugal, over the 1920–2004 period. The results revealed a set of oscillations with associated periods in the 2–3, 4–5 and 6–8 years bands, peaking at 6.5-year (Guadiana river) in the south of Portugal. They concluded that the overall relationship between NAO and river streamflow was complex and nonstationary. Spectral methods applied to a set of 53 piezometer time series from the Vega de Granada alluvial aquifer, in southern Spain, along with rainfall, temperature and river flow data, also identified cycles of 8–11 years and 3.2 years (Luque-Espinar et al., 2008). Also in agreement with previous studies, our results expose a stronger influence of NAO in the south of Portugal. Such dependence on geographic location was previously recognized in studies analyzing the impact of climate modes on Iberian lakes (Hernández et al., 2015), streamflow (Lorenzo-Lacruz et al., 2011) and wind speed (Correia et al., 2017) among others. However, few studies so far quantified the impact of EA or SCAND on Iberian hydrologic time series, despite the increasing awareness of their importance (Comas-Bru and Mcdermott, 2013; Steirou et al., 2017; Bastos et al., 2016).

Quantitative relationships between climate indices and precipitation obtained from individual weather stations demand cautious interpretation since precipitation time-series in Iberia may display notable differences even among neighboring locations. Nonetheless,

Table 2
Spearman's rank correlation coefficients between the winter (DJFM) climate indices and the seasonal aggregates of the wavelet principal components (PC1, PC2 and PC3) of the piezometric levels. Only significant correlations are shown.

Wavelet PCs (season)	Lavos			Carriço		
	NAO	EA	SCA	NAO	EA	SCA
PC1 winter	−0.44					
PC1 summer	−0.43					
PC2 summer		0.42	**0.54***			0.44
PC3 summer				−0.31	0.35	
Wavelet PCs (season)	**Silves**			**Benafim**		
	NAO	**EA**	**SCA**	**NAO**	**EA**	**SCA**
PC1 winter	**−0.63**			**−0.63**		
PC1 summer	**−0.60**			**−0.60**		
PC2 summer		0.40	0.47	−0.38		
PC3 summer	−0.38				0.40	**0.47**

* Bold and regular numbers indicate significance values at $p < 0.01$ and $p < 0.05$, respectively.

Table 3
Comparative results of the SSA and wPCA in the two aquifers. SSA: Periods of main modes of variability and contribution to the variance of groundwater levels. wPCA: variance explained by the first three wavelet principal components.

Leirosa-Monte Real				
SSA explained variance (%)			wPCA explained variance (%)	
Period (years)	Lavos	Carriço	Lavos	Carriço
> 10	17	31	PC1	PC1
10				
7.5	13			
6		23		
NAO [6, > 10]	30	54	36	55
4.2			PC2 + PC3	PC2 + PC3
3.3	26	25		
2.5	14	12		
EA + SCA [2.5,4.2]	40	37	43	38
Total	70	91	79	93
Querença-Silves				
SSA explained variance (%)			**wPCA explained variance (%)**	
Period (years)	**Silves**	**Benafim**	**Silves**	**Benafim**
> 10			PC1	PC1
10	64			
7.5		60		
6				
NAO [6, > 10]	64	60	54	53
4.2	20	24	PC2 + PC3	PC2 + PC3
3.3				
2.5				
EA + SCA [2.5,4.2]	20	24	36	33
Total	84	84	90	86

according to wavelet PCA results NAO, EA and SCAND (PC1 + PC2 + PC3) are responsible for 85% and 95% of the total variance of precipitation in the LM and QS aquifers, respectively (Fig. 8). Among them, NAO contributes to 64% and 74% of the variance in the north and south, respectively, in agreement with expected patterns for this teleconnection. The groundwater response to rainfall depends on evapotranspiration, land cover and geologic factors such as topography and soil permeability, which affect infiltration and recharge. These factors attenuate climate signals and may explain the relatively weaker impacts of climate indices on piezometric levels than on precipitation. In the QS aquifer for instance, geological filtering related to spatially heterogeneous geomorphologic and hydrogeologic properties (water storage capacity and transmissivity) accounts for 15% of differential variability in piezometric levels among eastern and western sectors (Neves et al., 2016). Rodriguez-Puebla et al. (1998) quantified the association between climate indices and precipitation at the Iberian scale based on an empirical orthogonal function analysis of precipitation from 51 meteorological stations, from 1949 to 1995. In spite of showing significant spatial variability their results indicate that on average EA accounts for 33% of the total variance of precipitation, while NAO and SCAND explain 19% and 13% of the total precipitation variance, respectively. Differences between these estimates and findings of the present study may be attributed to the local scale of our analysis, to the different methods employed and to the different time spans analyzed.

Perhaps the most interesting aspect of the present study, and novelty in what concerns to groundwater levels, is the recognition that transitive couplings among the indices (NAO, EA and SCAND) greatly affect hydrological responses. Coupled phases between climate modes may prompt extreme or anomalous precipitation events (Cleverly et al., 2016; Kalimeris et al., 2017) and indeed, our results provide evidence of an association between coupled NAO and EA phases and extremes in groundwater levels. Moreover, wavelet transform methods (WTC and wPCA) applied to groundwater levels clearly show that extreme events (droughts in Portugal) mark abrupt transitions in synchronization patterns among NAO, EA and SCAND. In future, integrated forecast system of groundwater availability can benefit from the identification of such abrupt transitions, which define time windows where it is possible to assume quasi-stationary behavior of climate patterns.

Understanding the response of hydrologic systems to atmospheric circulation modes is extremely important in the context of climate change. Groundwater plays a critical role for its value as a buffer system during droughts events and because it is very often the main source of potable water for irrigation (certainly in Portugal). The results of the present study may motivate future investigations focusing on the impacts of coupled climate patterns on aquifer levels and on the association of coupled phases with hydrologic extremes. For example, national scale assessments of the effects of teleconnections on aquifers across the USA and Canada showed that groundwater levels are controlled by interannual and multidecadal variability associated with the El Niño–Southern Oscillation, NAO, Pacific Decadal Oscillation, Atlantic Multidecadal Oscillation and Artic Oscillation (Kuss and Gurdak, 2014; Tremblay et al., 2011). However, from the point of view of the subsurface components of the water cycle, the interactions amongst climate patterns remain underestimated in North America. In the southern hemisphere, strong precipitation anomalies observed in Australia occur when teleconnections in the Pacific and Indian Oceans are synchronized (Cleverly et al., 2016) but the impact of such synchronization on aquifers still needs evaluation. Further investigation is also vital in India and East Africa, where groundwater storage depends heavily on extreme rainfall related to monsoon precipitation forced by the Indian Ocean Dipole and the El Niño–Southern Oscillation (Asoka et al., 2017; Taylor et al., 2013). Likewise, studies addressing the influence of long-term climate variability on groundwater recharge in Europe are scarce and focus only on individual teleconnections (Holman et al., 2011; De Vita et al., 2012). Groundwater simulations incorporating a priori knowledge about local hydroclimatic responses will globally help to improve resources planning and better prepare for climate changing scenarios. The sensitivity of aquifers to the propagation of climate signals depends not only on hydrogeological properties but also on the local dynamics of the climate patterns themselves, even at relatively small scales as exposed by the north-south asymmetry found in Portugal. Site-dependent studies are thus required in order to assess the vulnerability of groundwater supplies to long-term climate-induced

variations, particularly through its influence on precipitation and pumping.

As far as projections for the identified leading patterns of variability (NAO, EA and SCAND) becomes available and reliable, medium to long-term forecasts and inferences about groundwater levels states in Portugal could be attempted on an operational mode. Although no significant trends were detected in the analyzed period, neither for the climate indicators, nor in the piezometric levels series –which hampers an in-depth long-term trend analysis–, under future warmer climate conditions, recent researches have identified slight positive shifts in the probability distribution of the NAO phase (Barnes and Polvani, 2015; Deser et al., 2017; Woollings and Blackburn, 2012). Acknowledging that there is still a large uncertainty in these long-horizon predictions, and that the magnitude of the projected trends is well masked by the natural, predominantly stochastic, inter-annual oscillations of the NAO index (Deser et al., 2017), this would imply the risk of lower than current groundwater levels, on average. That scenario would demand corresponding efforts for the design and implementation of adaptation measures. In the medium range, these measures could take advantage of the progresses achieved for forecasting the NAO, and other teleconnection patterns, months (even one year) ahead (Brands et al., 2012; Dunstone et al., 2016; Scaife et al., 2014) along with the results reported here.

7. Conclusions

This study examines the teleconnections between NAO, EA, SCAND and precipitation and groundwater level fluctuations. In the particular aquifers considered here (Leirosa-Monte Real and Querença-Silves) precipitation and groundwater levels showed very similar responses to climate modes. However, monthly fluctuations in groundwater levels were smoother and showed more consistent links to climate indices than precipitation, which makes them useful to assist in developing process-based models (e.g. hindcast) of observed changes in the long-term.

The capacity of wavelet transform methods to analyze processes at various scales exposes not only the impacts of climate modes (NAO, EA and SCAND) on groundwater levels but also the existence of complex transitive couplings among modes. Extreme events coinciding with coupled phases (e.g. droughts and NAO + EA−) mark sharp boundaries in mode interaction patterns or sudden shifts in the time-frequency space. Groundwater levels over the analyzed time interval (1987–2016) display consistent relationships with climate indices in distinct period bands and time windows. The strongest covariability occurs in the 6–10 years band for NAO, in the 2–4 years band for EA (especially after 1999) and in the 4–6 years band for SCAND (especially after 2005). Episodes displaying simultaneously multiple coherent relationships are associated with coupled phases among NAO, EA and SCAND.

The contribution of each set of oscillations to the total variance of the groundwater levels was evaluated using singular spectral analysis and wavelet principal component analysis as complementary approaches. The results indicate that NAO, EA and SCAND patterns together are responsible for most (80%) of the inter-annual variability of groundwater levels in Portugal. NAO is the first leading pattern of variability, accounting for 40% and 60% of the total variance of groundwater levels in the north and south of the country, respectively. The joint contributions of EA and SCAND account for the remaining 40% of variability in the north and 20% of variability in the south, on average. Their individual contributions are difficult to distinguish but EA (associated with peak periods of 2.5 and 3.3 years) is relatively more influential in the north while SCAND (associated with peak periods of 4.2 years) is relatively more influential in the south.

Monthly groundwater levels averaged over years of positive and negative phases of climate indices provide additional insights. The impact of NAO alone is clear since lower (higher) groundwater levels occur during years of positive (negative) NAO phases. Moreover, extreme piezometric levels take place in years of anti-phase EA and NAO combinations. Combined winter NAO-EA+ phases are associated with maximum groundwater levels while combined NAO + EA− phases are associated with minimum levels.

Climate change projections of more frequent and severe droughts over the next decades will have challenging effects on groundwater demands. Further understanding on how climate modes influence groundwater storage, with particular emphasis on the implications of phase couplings and on their relationship to extreme events, will help to improve future projections of groundwater availability and guide integrated water resource management practices not only in Portugal but around the world.

Declarations of interest

None.

Acknowledgements

This work is supported by FCT-project UID/GEO/50019/2013 – IDL. Thanks to Pedro Viterbo who nicely provided the precipitation data from the IPMA meteorological stations and to Luis Costa and José P. Monteiro for useful discussions. The authors are also indebted to three anonymous reviewers for their constructive and thorough reviews of the manuscript.

References

Almeida, C., Mendonça, J.J.L., Jesus, M.R., Gomes, A.J., 2000. In: Sistema de aquíferos de Portugal continental, pp. 3–133.

Andreo, B., Jiménez, P., Durán, J.J., Carrasco, F., Vadillo, I., Mangin, A., 2006. Climatic and hydrological variations during the last 117–166 years in the south of the Iberian Peninsula, from spectral and correlation analyses and continuous wavelet analyses. J. Hydrol. 324, 24–39. https://doi.org/10.1016/j.jhydrol.2005.09.010.

Asoka, A., Gleeson, T., Wada, Y., Mishra, V., 2017. Relative contribution of monsoon precipitation and pumping to changes in groundwater storage in India. Nat. Geosci. 10, 109–117. https://doi.org/10.1038/ngeo2869.

Barnes, E.A., Polvani, L.M., 2015. CMIP5 projections of arctic amplification, of the North American/North Atlantic circulation, and of their relationship. J. Clim. 28, 5254–5271. https://doi.org/10.1175/JCLI-D-14-00589.1.

Barnston, A.G., Livezey, R.E., 1987. Classification, seasonality and persistence of low-frequency atmospheric circulation patterns. Mon. Weather Rev. 115, 1083–1126. https://doi.org/10.1175/1520-0493(1987) 115<1083:CSAPOL>2.0.CO;2.

Bastos, A., Janssens, I.A., Gouveia, C.M., Trigo, R.M., Ciais, P., Chevallier, F., Peñuelas, J., Rödenbeck, C., Piao, S., Friedlingstein, P., Running, S.W., 2016. European land CO_2 sink influenced by NAO and east-atlantic pattern coupling. Nat. Commun. 7. https://doi.org/10.1038/ncomms10315.

Belo-Pereira, M., Dutra, E., Viterbo, P., 2011. Evaluation of global precipitation data sets over the Iberian Peninsula. J. Geophys. Res. Atmos. 116, 1–16. https://doi.org/10.1029/2010JD015481.

Brands, S., Manzanas, R., Gutiérrez, J.M., Cohen, J., 2012. Seasonal predictability of wintertime precipitation in Europe using the snow advance index. J. Clim. 25, 4023–4028. https://doi.org/10.1175/JCLI-D-12-00083.1.

Bueh, C., Nakamura, H., 2007. Scandinavian pattern and its climatic impact. Q. J. R. Meteorol. Soc. 133, 2117–2131. https://doi.org/10.1002/qj.173.

Cleverly, J., Eamus, D., Luo, Q., Coupe, N.R., Kljun, N., Ma, X., Ewenz, C., Li, L., Yu, Q., Huete, A., 2016. The importance of interacting climate modes on Australia's contribution to global carbon cycle extremes. Sci. Rep. 6, 1–10. https://doi.org/10.1038/srep23113.

Comas-Bru, L., Mcdermott, F., 2013. Impacts of the EA and SCA patterns on the European twentieth century NAO-winter climate relationship. Q. J. R. Meteorol. Soc. 140, 354–363. https://doi.org/10.1002/qj.2158.

Correia, J.M., Bastos, A., Brito, M.C., Trigo, R.M., 2017. The influence of the main large-scale circulation patterns on wind power production in Portugal. Renew. Energy 102, 214–223. https://doi.org/10.1016/j.renene.2016.10.002.

Daubechies, I., 1990. The wavelet transform, time-frequency localization and signal analysis. Inf. Theory, IEEE Trans. 36, 961–1005. https://doi.org/10.1109/18.57199.

De Vita, P., Allocca, V., Manna, F., Fabbrocino, S., 2012. Coupled decadal variability of the North Atlantic Oscillation, regional rainfall and karst spring discharges in the Campania region (southern Italy). Hydrol. Earth Syst. Sci. 16, 1389–1399. https://doi.org/10.5194/hess-16-1389-2012.

Deser, C., Hurrell, J.W., Phillips, A.S., 2017. The role of the North Atlantic Oscillation in European climate projections. Clim. Dyn. 49, 3141–3157. https://doi.org/10.1007/

s00382-016-3502-z.
Dettinger, M.D., Ghil, M., Strong, C.M., Weibel, W., Yiou, P., 1995. Software expedites singular-spectrum analysis of noisy time series. Eos (Washington. DC). 76, 12, 14, 21.
Dickinson, J.E., Ferré, T.P.A., Bakker, M., Crompton, B., 2014. A screening tool for delineating subregions of steady recharge within groundwater models. Vadose Zo. J. 13. https://doi.org/10.2136/vzj2013.10.0184.
Dickinson, J.E., Hanson, R.T., Ferré, T.P.A., Leake, S.A., 2004. Inferring time-varying recharge from inverse analysis of long-term water levels. Water Resour. Res. 40, W07403. https://doi.org/10.1029/2003WR002650.
Dunstone, N., Smith, D., Scaife, A., Hermanson, L., Eade, R., Robinson, N., Andrews, M., Knight, J., 2016. Skilful predictions of the winter North Atlantic Oscillation one year ahead. Nat. Geosci. 9, 809–814. https://doi.org/10.1038/ngeo2824.
ECMWF, 2017. European Centre for Medium-Range Weather Forecasts [WWW Document]. URL https://www.ecmwf.int/en/forecasts/datasets/reanalysis-datasets/era-interim.
García-Herrera, R., Hernández, E., Barriopedro, D., Paredes, D., Trigo, R.M., Trigo, I.F., Mendes, M.A., 2007. The outstanding 2004/05 drought in the iberian peninsula: associated atmospheric circulation. J. Hydrometeorol.
Gámiz-Fortis, S.R., 2002. Spectral characteristics and predictability of the NAO assessed through Singular Spectral Analysis. J. Geophys. Res. 107, 4685. https://doi.org/10.1029/2001JD001436.
Ghil, M., Allen, M.R., Dettinger, M.D., Ide, K., Kondrashov, D., Mann, M.E., Robertson, A.W., Saunders, A., Tian, Y., Varadi, F., Yiou, P., 2002. Advanced spectral methods for climatic time series. Rev. Geophys. 40, 1–41. https://doi.org/10.1029/2001RG000092.
Grinsted, A., Moore, J.C., Jevrejeva, S., 2004. Application of the cross wavelet transform and wavelet coherence to geophysical time series. Nonlinear Process. Geophys. 11, 561–566. https://doi.org/10.5194/npg-11-561-2004.
Guerreiro, S.B., Birkinshaw, S., Kilsby, C., Fowler, H.J., Lewis, E., 2017a. Dry getting drier – the future of transnational river basins in Iberia. J. Hydrol. Reg. Stud. 12, 238–252. https://doi.org/10.1016/j.ejrh.2017.05.009.
Guerreiro, S.B., Kilsby, C., Fowler, H.J., 2017b. Assessing the threat of future mega-drought in Iberia. Int. J. Climatol. 37, 5024–5034. https://doi.org/10.1002/joc.5140.
Gurdak, J.J., Hanson, R.T., McMahon, P.B., Bruce, B.W., McCray, J.E., Thyne, G.D., Reedy, R.C., 2007. Climate Variability Controls on Unsaturated Water and Chemical Movement. Vadose Zo. J, High Plains Aquifer, USA.
Hanson, R.T., Newhouse, M.W., Dettinger, M.D., 2004. A methodology to asess relations between climatic variability and variations in hydrologic time series in the southwestern United States. J. Hydrol. 287, 252–269. https://doi.org/10.1016/j.jhydrol.2003.10.006.
Hernández, A., Trigo, R.M., Pla-Rabes, S., Valero-Garcés, B.L., Jerez, S., Rico-Herrero, M., Vega, J.C., Jambrina-Enríquez, M., Giralt, S., 2015. Sensitivity of two Iberian lakes to North Atlantic atmospheric circulation modes. Clim. Dyn. 45, 3403–3417. https://doi.org/10.1007/s00382-015-2547-8.
Holman, I.P., Rivas-Casado, M., Bloomfield, J.P., Gurdak, J.J., 2011. Identifying non-stationary groundwater level response to North Atlantic ocean-atmosphere teleconnection patterns using wavelet coherence. Hydrogeol. J. 19, 1269–1278. https://doi.org/10.1007/s10040-011-0755-9.
Hugman, R., Stigter, T., Costa, L., Monteiro, J.P., 2017. Numerical modelling assessment of climate-change impacts and mitigation measures on the Querença-Silves coastal aquifer (Algarve, Portugal). Hydrogeol. J. 2105–2121. https://doi.org/10.1007/s10040-017-1594-0.
Hugman, R., Stigter, T.Y., Monteiro, J.P., Nunes, L., 2012. Influence of aquifer properties and the spatial and temporal distribution of recharge and abstraction on sustainable yields in semi-arid regions. Hydrol. Process. 26, 2791–2801. https://doi.org/10.1002/hyp.8353.
Hurrell, J.W., Kushnir, Y., Ottersen, G., Visbeck, M., 2003. An Overview of the North Atlantic Oscillation. North Atl. Oscil Clim. Significance Environ. Impact Geophys. Monogr. 134, 1–35. https://doi.org/10.1029/134GM01.
Hurrell, J.W., Van Loon, H., 1997. Decadal variatons in climate associated with the North Atlantic Oscillation. Clim. Chang. 36, 301–326.
IPMA, 2017. Instituto Português do Mar a e da Atmosfera [WWW Document]. Port. Inst. Sea Atmos. URL.
Jerez, S., Trigo, R.M., 2013. Time-scale and extent at which large-scale circulation modes determine the wind and solar potential in the Iberian Peninsula. Environ. Res. Lett. 8, 44035. https://doi.org/10.1088/1748-9326/8/4/044035.
Jerez, S., Trigo, R.M., Vicente-Serrano, S.M., Pozo-Vázquez, D., Lorente-Plazas, R., Lorenzo-Lacruz, J., Santos-Alamillos, F., Montávez, J.P., 2013. The impact of the north atlantic oscillation on renewable energy resources in Southwestern Europe. J. Appl. Meteorol. Climatol. 52, 2204–2225. https://doi.org/10.1175/JAMC-D-12-0257.1.
Kalimeris, A., Ranieri, E., Founda, D., Norrant, C., 2017. Variability modes of precipitation along a Central Mediterranean area and their relations with ENSO, NAO, and other climatic patterns. Atmos. Res. 198, 56–80. https://doi.org/10.1016/j.atmosres.2017.07.031.
Katul, G.G., Parlange, M.B., 1995. The spatial structure of turbulence at production wavenumbers using orthonormal wavelets. Boundary-Layer Meteorol. 75, 81–108. https://doi.org/10.1007/BF00721045.
Kuss, A.J.M., Gurdak, J.J., 2014. Groundwater level response in U.S. principal aquifers to ENSO, NAO, PDO, and AMO. J. Hydrol. 519, 1939–1952. https://doi.org/10.1016/j.jhydrol.2014.09.069.
Lorenzo-Lacruz, J., Moŕan-Tejeda, E., Vicente-Serrano, S.M., Ĺopez-Moreno, J.I., 2013. Streamflow droughts in the Iberian Peninsula between 1945 and 2005: Spatial and temporal patterns. Hydrol. Earth Syst. Sci. 17, 119–134. https://doi.org/10.5194/hess-17-119-2013.
Lorenzo-Lacruz, J., Vicente-Serrano, S.M., López-Moreno, J.I., González-Hidalgo, J.C., Morán-Tejeda, E., 2011. The response of Iberian rivers to the North Atlantic Oscillation. Hydrol. Earth Syst. Sci. 15, 2581–2597. https://doi.org/10.5194/hess-15-2581-2011.
Luque-Espinar, J.A., Chica-Olmo, M., Pardo-Igúzquiza, E., García-Soldado, M.J., 2008. Influence of climatological cycles on hydraulic heads across a Spanish aquifer. J. Hydrol. 354, 33–52. https://doi.org/10.1016/j.jhydrol.2008.02.014.
Martins, D.S., Raziei, T., Paulo, A.A., Pereira, L.S., 2012. Spatial and temporal variability of precipitation and drought in Portugal. Nat. Hazards Earth Syst. Sci. 12, 1493–1501. https://doi.org/10.5194/nhess-12-1493-2012.
Miranda, P., Coelho, F.E.S., Tomé, A.R., Valente, M.A., 2002. 20th century Portuguese climate and climate scenarios. In: Climate Change in Portugal. Scenarios, Impacts and Adaptation Measures. SIAMproject, pp. 23–83.
Monteiro, J., 2006. Inverse calibration of a regional flow model for the Querença-Silves Aquifer System (Algarve- Portugal). In: Proceedings of the International Congress on Integrated Water Resources Management and Challenges of the Sustainable. Marakesh, Morocco, pp. 44.
Moore, G.W.K., Renfrew, I.A., Pickart, R.S., 2013. Multidecadal mobility of the north atlantic oscillation. J. Clim. 26, 2453–2466. https://doi.org/10.1175/JCLI-D-12-00023.1.
Moreno, J., Fatela, F., Gonçalves, M.A., Leorri, E., Trigo, R.M., Moreno, F., Gómez-Navarro, J.J., Brázdil, R., Ferreira, M.J., 2018. Climate reconstruction for the Entre-Douro-e-Minho region (NW Portugal) between AD 1626 and AD 1820: synthesis of viticulture data and foraminiferal evidence. Boreas. https://doi.org/10.1111/bor.12331.
Neves, M.C., Costa, L., Monteiro, J.P., 2016. Climatic and geologic controls on the piezometry of the Querença-Silves karst aquifer, Algarve (Portugal). Hydrogeol. J. 24. https://doi.org/10.1007/s10040-015-1359-6.
NOAA, 2017. National Oceanic and Atmospheric Administration, Climate Preciction. Center [WWW Document].
Ribeiro, L., da Cunha, L.V., 2010. Portuguese Groundwater Report – Easac Wg on the Role of Groundwater in the Water Resources Policy of. Southern Eu Member States.
Rodriguez-Puebla, C., Encinas, A.H., Nieto, S., Garmendia, J., 1998. Spatial and temporal patterns of annual precipitation variability over the Iberian Peninsula. Int. J. Climatol. 18, 299–316. https://doi.org/10.1002/(SICI)1097-0088(19980315)18:3<299::AID-JOC247>3.0.CO;2-L.
Sang, Y.-F., 2013. A review on the applications of wavelet transform in hydrology time series analysis. Atmos. Res. 122, 8–15. https://doi.org/10.1016/j.atmosres.2012.11.003.
Scaife, A.A., Arribas, A., Blockley, E., Brookshaw, A., Clark, R.T., Dunstone, N., Eade, R., Fereday, D., Folland, C.K., Gordon, M., Hermanson, L., Knight, J.R., Lea, D.J., MacLachlan, C., Maidens, A., Martin, M., Peterson, A.K., Smith, D., Vellinga, M., Wallace, E., Waters, J., Williams, A., 2014. Skillful long-range prediction of European and North American winters. Geophys. Res. Lett. 41, 2514–2519. https://doi.org/10.1002/2014GL059637.
SNIRH, 2017. Sistema Nacional de Informação de Recursos Hídricos [WWW Document]. Natl. Inf. Syst. Water Resour.
Steirou, E., Gerlitz, L., Apel, H., Merz, B., 2017. Links between large-scale circulation patterns and streamflow in Central Europe: A review. J. Hydrol. 549, 484–500. https://doi.org/10.1016/j.jhydrol.2017.04.003.
Stigter, T.Y., Nunes, J.P., Pisani, B., Fakir, Y., Hugman, R., Li, Y., Tomé, S., Ribeiro, L., Samper, J., Oliveira, R., Monteiro, J.P., Silva, a., Tavares, P.C.F., Shapouri, M., Cancela da Fonseca, L., El Himer, H., 2014. Comparative assessment of climate change and its impacts on three coastal aquifers in the Mediterranean. Reg. Environ. Chang. 14, 41–56. https://doi.org/10.1007/s10113-012-0377-3.
Sun, Q., Miao, C., Duan, Q., Ashouri, H., Sorooshian, S., Hsu, K.L., 2018. A review of global precipitation data sets: data sources, estimation, and intercomparisons. Rev. Geophys. 56, 79–107. https://doi.org/10.1002/2017RG000574.
Taylor, R.G., Scanlon, B., Döll, P., Rodell, M., Van Beek, R., Wada, Y., Longuevergne, L., Leblanc, M., Famiglietti, J.S., Edmunds, M., Konikow, L., Green, T.R., Chen, J., Taniguchi, M., Bierkens, M.F.P., Macdonald, A., Fan, Y., Maxwell, R.M., Yechieli, Y., Gurdak, J.J., Allen, D.M., Shamsudduha, M., Hiscock, K., Yeh, P.J.F., Holman, I., Treidel, H., 2013. Ground water and climate change. Nat. Clim. Chang. 3, 322–329. https://doi.org/10.1038/nclimate1744.
Torrence, C., Compo, G.P., 1998. A Practical Guide to Wavelet Analysis. Bull. Am. Meteorol. Soc. 79, 61–78.
Torrence, C., Webster, P.J., 1998. The annual cycle of persistence in the El Nino/Southern Oscillation. Q. J. R. Meteorol. Soc. 124, 1985–2004. https://doi.org/10.1002/qj.49712455010.
Tremblay, L., Larocque, M., Anctil, F., Rivard, C., 2011. Teleconnections and interannual variability in Canadian groundwater levels. J. Hydrol. 410, 178–188. https://doi.org/10.1016/j.jhydrol.2011.09.013.
Trigo, R.M., Añel, J.A., Barriopedro, D., García-Herrera, R., Gimeno, L., Nieto, R., Castillo, R., Allen, M.R., Massey, N., 2013. The record winter drought of 2011–12 in the Iberian peninsula. Bull. Am. Meteorol. Soc.
Trigo, R.M., Palutikof, J.P., 2001. Precipitation scenarios over Iberia: A comparison between direct GCM output and different downscaling techniques. J. Clim. 14, 4422–4446. https://doi.org/10.1175/1520-0442(2001) 014<4422:PSOIAC>2.0.CO;2.
Trigo, R.M., Pozo-Vázquez, D., Osborn, T.J., Castro-Díez, Y., Gámiz-Fortis, S., Esteban-Parra, M.J., 2004. North Atlantic oscillation influence on precipitation, river flow and water resources in the Iberian Peninsula. Int. J. Climatol. 24, 925–944. https://doi.org/10.1002/joc.1048.
Trigo, R.M., Valente, M.a., Trigo, I.F., Miranda, P.M.a., Ramos, A.M., Paredes, D., García-Herrera, R., 2008. The impact of North Atlantic wind and cyclone trends on European precipitation and significant wave height in the Atlantic. Trends Dir. Clim. Res. Ann. N.Y Acad. Sci. 1146, 212–234. https://doi.org/10.1196/annals.1446.014.

Vautard, R., Yiou, P., Ghil, M., 1992. Singular-spectrum analysis: A toolkit for short, noisy chaotic signals. Phys. D Nonlinear Phenom.

Velasco, E.M., Gurdak, J.J., Dickinson, J.E., Ferré, T.P.A., Corona, C.R., 2017. Interannual to multidecadal climate forcings on groundwater resources of the U.S. West Coast. J. Hydrol. Reg. Stud. 11, 250–265. https://doi.org/10.1016/j.ejrh.2015.11.018.

Venencio, M.D.V., García, N.O., 2011. Interannual variability and predictability of water table levels at Santa Fe Province (Argentina) within the climatic change context. J. Hydrol. 409, 62–70. https://doi.org/10.1016/j.jhydrol.2011.07.039.

Vicente-Serrano, S.M., López-Moreno, J.I., 2008. Nonstationary influence of the North Atlantic Oscillation on European precipitation. J. Geophys. Res. Atmos. 113.

Woollings, T., Blackburn, M., 2012. The north Atlantic jet stream under climate change and its relation to the NAO and EA patterns. J. Clim. 25, 886–902. https://doi.org/10.1175/JCLI-D-11-00087.1.

Zubiate, L., McDermott, F., Sweeney, C., O'Malley, M., 2017. Spatial variability in winter NAO–wind speed relationships in Western Europe linked to concomitant states of the East Atlantic and Scandinavian patterns. Q. J. R. Meteorol. Soc. 143, 552–562. https://doi.org/10.1002/qj.2943.